PAPER

Modulation of band gap by an applied electric field in silicene-based hetero-bilayers†

Sandeep Nigam,*[ab] Sanjeev K. Gupta,[ac] C. Majumder[b] and Ravindra Pandey*[a]

Electronic properties of the hetero-structures consisting of silicene, graphene and BN monolayers under the influence of an electric field were investigated using density functional theory. With no electric field, both silicene/graphene and silicene/BN were shown to have a finite gap of about $\sim$50 meV, though silicene is a zero-gap two-dimensional material. Application of the field perpendicular to the bilayer system was found to facilitate modulation of the band gap, exhibiting an approximately linear relationship with the gap energy, in contrast to what was seen for the constituent monolayers. Also, the degree of the modulation was mainly determined by the Si-p_z electronic states at the interface of the silicene/graphene and silicene/BN bilayers.

1. Introduction

Atomic layers with reduced dimensionality have been of great interest due to their unique and novel properties, which can be exploited for the next-generation electronic devices.[1–6] Modulation of band gap with the help of geometrical strain or external electric field makes the two-dimensional layers particularly interesting materials for device applications on the nanoscale.[7–15] For example, monolayer graphene remains a zero-gap material under an external electric field but a finite band gap appears for bilayer and multi-layer graphene.[11,12]

Besides graphene, other group IV elements, such as silicon has stable honeycomb monolayers referred to as silicene.[16–22] However, unlike graphene, silicene is stable only if a small buckling ($\approx$0.44 Å) is present,[17–19] though the electronic properties of silicene in both sheet and nanoribbon forms have been found to be similar to those of graphene.[23] The buckled nature of silicene has led to novel properties such as a spin Hall effect,[24,25] adsorption of dopant atoms,[26,27] and modulation of its band gap under an external electric-field.[17,18,28] Additionally, it may also be used to influence the dispersion of electrons in graphene in a bilayer system.[29] This phenomenon is similar to what has been demonstrated for the boron nitride (BN) monolayer, which induces a finite gap in graphene.[13–15] In this paper we will examine the extent of variation in the electronic

properties of silicene induced by the BN monolayer in a hetero bilayer system. We will also investigate the possible modulation of band gap of silicene in the hetero bilayer system under the application of external electric field. Considering that graphene is structurally similar to a BN monolayer, we planned to investigate the silicene/graphene bilayer system under the influence of the electric field. Calculations will also be performed on the graphene bilayer and the graphene/BN bilayer systems with an aim to rationalize the physics and chemistry of a heterogeneous bilayer in comparison to a homogenous bilayer system.

2. Computational method

Electronic structure calculations were performed using the plane-wave-based pseudopotential approach as implemented in the Vienna Ab initio Simulation Package (VASP).[30,31] The electron–ion interaction was described by the projector augmented wave (PAW) method,[32] and the Perdew–Burke–Ernzerhof (PBE) genera-lized gradient approximation was used.[33] The vdW correction (DFT-D2) within the PBE functional proposed by Grimme was also employed.[34] A vacuum distance of 15 Å was used in the supercell model. The cut-off energy for the plane wave basis set was fixed at 520 eV. The positions of atoms were optimized until the convergence of the force on each atom was less than 0.01 eV Å^{-1}. The total energy convergence was tested with respect to the plane-wave basis set size and the cell size leading its accuracy to be within 1 meV. The Monkhorst–Pack scheme was used to sample the Brillouin zone with 15 × 15 × 1 k-mesh.

The modeling parameters employed have reproduced the results of the previous studies on graphene,[13,35] silicene[18,19,35] and the BN monolayer,[36,37] demonstrating their accuracy and reliability to model 2D systems. For example, the lattice constants

^{a} *Department of Physics, Michigan Technological University, Houghton, Michigan, 49931, USA. E-mail: snigam.jpr@gmail.com, pandey@mtu.edu*

^{b} *Chemistry Division, Bhabha Atomic Research Centre, Trombay, Mumbai, 400085, India*

^{c} *Department of Physics and Electronics, St. Xavier's College Ahmedabad, India 380009*

of graphene, BN monolayer and silicene were calculated to be 2.47, 2.51 and 3.85 Å, respectively. Furthermore, the buckling of silicene (measured from the vertical distance between the two sub-lattices) was calculated to be 0.47 Å, in agreement with the previous[18,19] results based on density functional theory. A comparison of the values obtained by the present method with the previously reported values using the different method is presented in Table S1 of ESI.†

3. Results and discussion

3.1 Stability, structural and electronic properties

Fig. 1 shows the equilibrium configurations of the heterogeneous bilayers with six Si atoms located over the middle of C–C or B–N bonds and the other two Si atoms remaining over the hollow site of the hexagon of graphene or BN monolayer. Considering that the lattice mismatch of silicene with the graphene or BN monolayer is substantially large, we consider a co-periodic lattice to simulate the hetero-structure system. Application of a co-periodic lattice consisting of a (2×2) supercell of silicene with a (3×3) supercell of graphene or BN yielded a lattice mismatch of about 3%.

The structural parameters of the equilibrium configurations of the silicene/graphene and silicene/BN bilayers are given in Table 1. The intra-planar Si–Si bond was determined to be 2.27 Å in silicene, and nearly the same in the bilayers. On the other hand, the buckled height of the supported silicene slightly changed with regards to the pristine silicene; the average buckling values for silicene, silicene/graphene and silicene/BN bilayers were calculated to be 0.47, 0.60 and 0.54 Å, respectively. The interlayer distances ($R_{\text{interlayer}}$) for silicene/graphene and silicene/BN were calculated to be 3.36 and 3.32 Å, respectively. These values are similar to the 3.25 Å $R_{\text{interlayer}}$ calculated for the AB-stacked graphene bilayer and a bit larger than the 3.13 Å $R_{\text{interlayer}}$ calculated for the AB-stacked graphene/BN

Table 1   Stability and structural properties of the monolayer and bilayers studied

System	Intra-planar distance $R_{\text{intraplaner}}$ (Å)	Interlayer separation $R_{\text{interlayer}}$ (Å)	Binding energy (meV per atom)	Band gap (meV)
Silicene/graphene	$R_{\text{Si–Si}} = 2.23$ $R_{\text{C–C}} = 1.44$	3.36	13	51
Silicene/BN	$R_{\text{Si–Si}} = 2.24$ $R_{\text{B–N}} = 1.46$	3.32	24	47
Silicene	$R_{\text{Si–Si}} = 2.27$	—	—	~ 0
Graphene	$R_{\text{C–C}} = 1.43$	—	—	~ 0
BN monolayer	$R_{\text{B–N}} = 1.46$	—	—	~ 4500

bilayer. Previously, Cai *et al.* reported an interlayer separation of 3.3 Å with a band gap of about 57 meV for silicene/graphene at the LDA-DFT level of theory.[29]

The binding energy per atom with respect to the constituent monolayers (*i.e.*, $E_{\text{binding}} = E_{\text{A}} + E_{\text{B}} - E_{\text{AB}}$) was calculated to be 13 and 24 meV per atom for the silicene/graphene and silicene/BN bilayers, respectively, suggesting a stronger interlayer bonding between the silicene and BN than between the silicene and graphene. This small, but noticeable difference can be attributed to the degree of buckling in the hetero-bilayers; the strain energy was estimated to be 13 and 4 meV for silicene/graphene and silicene/BN, respectively [see ESI,† Table S2]. Note that the calculated binding energy for the AB-stacked graphene bilayer is 25 meV per atom whereas that of AB-stacked graphene/BN bilayer is 26 meV per atom. The h-BN monolayer has a finite band gap, and silicene and graphene are zero-gap materials. We found an opening of the band gap to 51 meV in the silicene/graphene bilayer, as was also previously reported,[29] and a finite band gap for the silicene/BN bilayer of 47 meV (Table 1).

Interatomic interactions plays crucial role in modulating the physical properties of nanostructures.[38] In order to gain further insight about the interlayer interactions, we examined the charge density of the bilayers at the interface (Fig. 2). Here, we observed a finite overlap of charge density contours for the three Si atoms located atop the substrate sites (graphene or BN), but a nearly zero charge density at the interface for the fourth Si atom, located at the hollow site of the substrate. On the other hand, the graphene bilayer system does not show such overlap, thus revealing the importance of the buckled nature of silicene with sp³-like characteristics in inducing the gap for the heterogeneous bilayer system.

3.2 Application of external electric field

Fig. 3 shows, for each of two heterogeneous bilayers, the dependence of its band gap energy on the strength of an applied external perpendicular electric field (E_{Field}) in the range of −0.4 to 0.4 V Å^{-1}. The positive value refers to the application of the electric field from the bottom to the top of the multilayer system. For our case, application of the field, which causes a redistribution of charges, is not likely to lead to structural changes. We note that Ni *et al.*[17] reported that an electric field of 0.5 V Å^{-1} changed the buckling of silicene by only 0.005 Å. Furthermore, Drummond and co-workers[18] showed that the
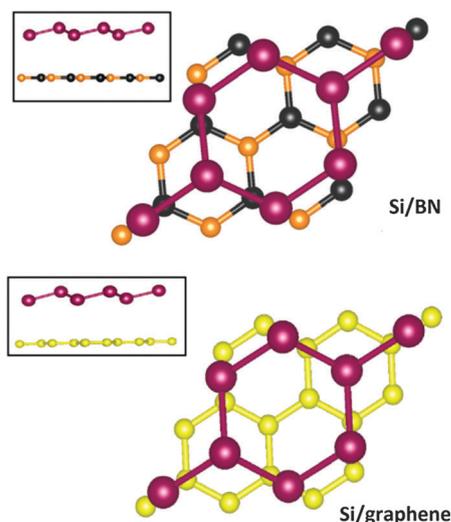

Fig. 1   Top view of the hetero bilayers: silicene/graphene and silicene/BN. (Si: purple, C: yellow, B: black, N: orange).
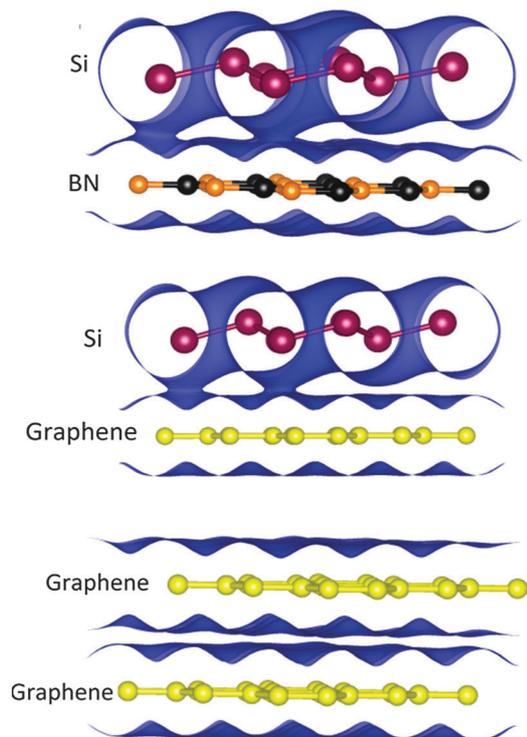
Fig. 2 The charge density contour of silicene/BN, silicene/graphene and graphene/graphene bilayers. The contour value is 0.001 electron per bohr^3.
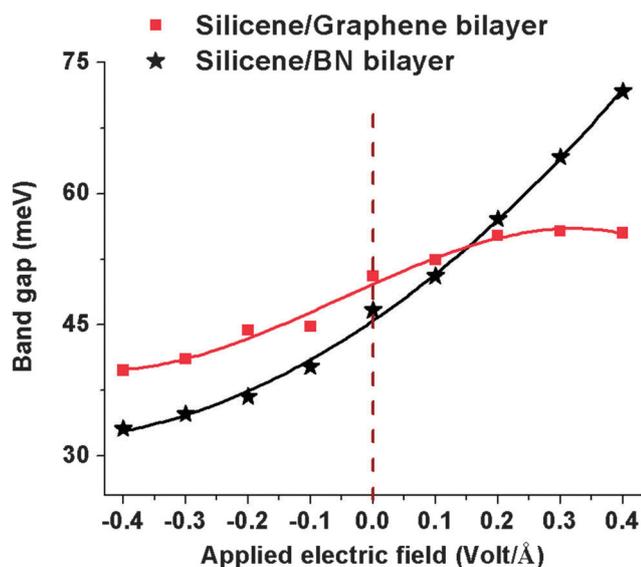

Fig. 3 Variation of the band gap energy with the strength of the perpendicular electric field.

silicene remains stable without any imaginary frequency in the phonon spectrum for the electric field of ~ 0.5 V Å^{-1}.

The silicene/graphene and silicene/BN bilayers exhibited roughly linear relationships between band gap energy and E_{Field} for E_{Field} values between -0.4 and 0.4 V Å^{-1}. This relationship is significantly different from that seen for the constituent monolayers; specifically for zero-gap silicene and graphene

[see ESI,† Fig. S1]. Furthermore, silicene/graphene and silicene/BN bilayers showed an asymmetric response to the electric field due to the presence of structural asymmetry in the heterogeneous bilayers (Fig. 3). It is well known that a symmetric response of a graphene bilayer to E_{Field} occurs when the constituent monolayers are structurally similar [see ESI,† Fig. S2]. Even though both silicene/ graphene and silicene/BN bilayers showed an asymmetric response to the electric field, the amount of modulation of the bandgap was found to be greater in the case of the silicene/BN bilayers. Graphene is structurally similar to a BN monolayer, but it is a symmetrical layered structure, whereas the symmetry is broken for BN (one sub-lattice consists of boron atoms, the other of nitrogen). Pandey and co-workers[14,15] have shown that the broken symmetry of BN is the cause of a larger opening of the band gap of graphene/BN bilayer under an electric field. Likewise, a higher band gap opening was predicted for silicene/BN bilayers in the present study.

Analysis of density of states (DOS) together with the charge density was also performed to gain insight into the response of the hetero-bilayers to the electric field. Fig. 4 shows the projected DOS of the p_z orbitals (perpendicular to the plane) for silicene/BN. Here, the Si-p_z states contributed near the Fermi level, and the band gap was estimated to be 47 meV. Under the influence of the electric field, a noticeable shift in the p_z bands associated with BN was seen to induce a significant variation in the band gap of the hetero-bilayers (Fig. 3). This was also shown to be the case with the graphene/BN bilayer where the p_z states associated with BN shifts under the influence of the electric field [see ESI,† Fig. S3].
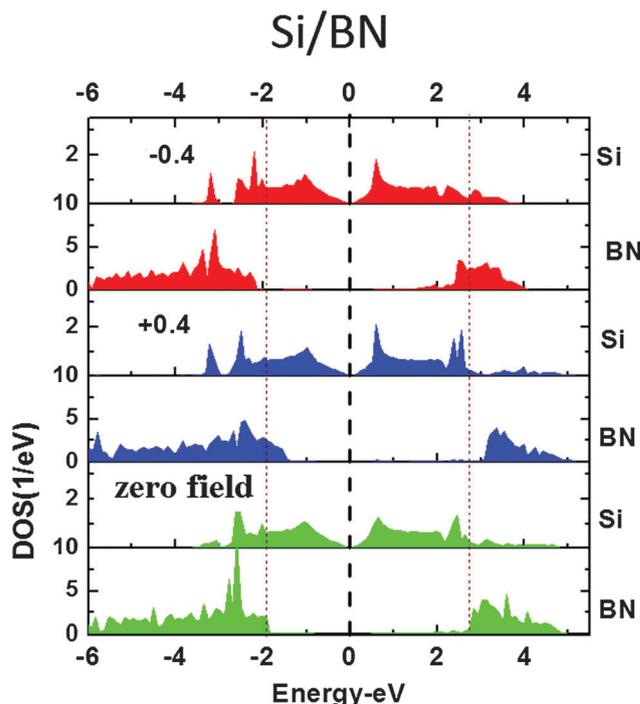

Fig. 4 The p_z orbital projected density of states for silicene/BN for $E_{\text{Field}} = 0$, $+0.4$ V Å^{-1}, and -0.4 V Å^{-1}. Zero of the energy scale is aligned to the Fermi level. The dotted line corresponds to the top of the valance band and bottom of the conduction band of the BN monolayer layer at $E_{\text{Field}} = 0$.
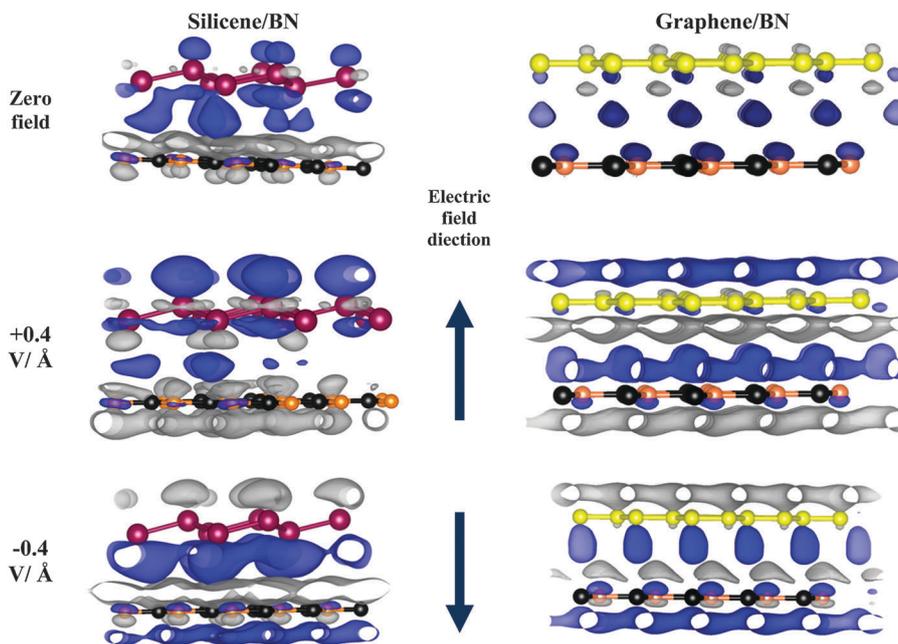
Fig. 5 The charge density difference ($\Delta\rho$) of silicene/BN and graphene/BN bilayers for E_{Field} = 0, +0.4 V Å^{-1}, and −0.4 V Å^{-1} using 6×10^{-3} electron per bohr^3 contours. Blue shows an increase in the charge density, and gray shows a decrease in the charge density.

Fig. 5 displays the charge density difference ($\Delta\rho$) for silicene/BN, which is defined as $\Delta\rho = \rho(\text{silicene/BN}) - \rho(\text{silicene}) - \rho(\text{BN})$. Here, $\rho(\text{silicene/BN})$ is the charge density of the hetero bilayer system. $\rho(\text{silicene})$ and $\rho(\text{BN})$ are the charge densities of the silicene and BN monolayers, respectively. Fig. 5 also includes $\Delta\rho$ for the graphene/BN bilayer system to bring out the subtleties in the physics and chemistry of silicene/BN with reference to graphene/BN. The charge density difference contours for silicene/graphene and graphene bilayers are given elsewhere [see ESI,† Fig. S4].

The significant difference in the charge density at the interface of silicene/BN with that of graphene/BN can be attributed to the fact that (i) Si atom is relatively more polarizable than carbon and (ii) buckled nature of the silicene monolayer. Note that the values of static dipole polarizability of C, B, N and Si were reported[39,40] to be 11.6, 20.43, 7.26 and 37.4 a.u., respectively. Application of an electric field induces redistribution of the charge density over Si and N atoms of the silicene/BN bilayer, which is much more localized in nature than that seen for graphene/BN or graphene bilayer systems.

Since the electronic properties of the silicene/BN bilayer are governed by the electronic properties of silicene, we investigated a system in which a silicene monolayer is deposited on the h-BN substrate. Electronic structure calculations for silicene deposited on the AA′ stacked h-BN multilayers yielded an interlayer distance between silicene and the top layer of the substrate of 3.31 Å with a binding energy of about 31 meV per atom. The h-BN substrate is represented in our model by a slab consisting of 5 BN layers with an interlayer distance of 3.1 Å. Fig. 6 compares the response of the electric field for silicene/BN and silicene/BN substrate, and shows the modulation of the heterogeneous system indeed being governed by the
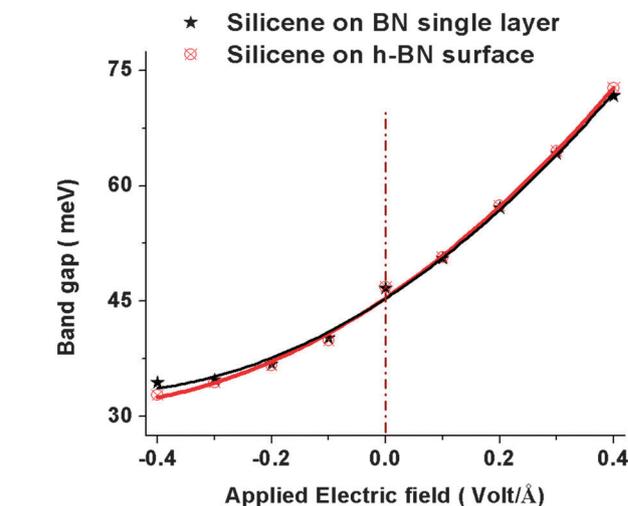

Fig. 6 Variation of the band gap energy with the strength of the perpendicular electric field.

electronic properties of silicene *via* Si-p$_z$ states at the interface (see ESI,† Fig. S5).

4. Summary

Electronic structure calculations were performed to investigate the stability and electronic properties of the bilayers consisting of silicene, graphene and BN. Application of the external electric field was found to modulate the band gap of the heterogeneous bilayers. A comparison of the calculated results on silicene/graphene and silicene/BN with the graphene/BN bilayer suggests that the interface electronic structure is dominated by Si-p$_z$

states that determine the electronic properties of the heterogeneous bilayers that we used. We believe that the results of our study will help advance the fundamental understanding of silicene-based two-dimensional materials so that they may be incorporated in next-generation microelectronics.

Acknowledgements

References

1 A. H. Castro Neto, F. Guinea, N. M. R. Peres, K. S. Novoselov and A. K. Geim, *Rev. Mod. Phys.*, 2009, **81**, 109.

2 K. Geim, *Science*, 2009, **324**, 1530.

3 L. Liu and Z. Shen, *Appl. Phys. Lett.*, 2009, **95**, 252104.

4 A. Lherbier, X. Blase, Y. Niquet, F. Triozon and S. Roche, *Phys. Rev. Lett.*, 2008, **101**, 036808.

5 F. Yavari, C. Kritzinger, C. Gaire, L. Song, H. Gullapalli, T. Borca-Tasciuc, P. M. Ajayan and N. Koratkar, *Small*, 2010, **6**, 2535.

6 D. Xu, H. He, R. Pandey and S. P. Karna, *J. Phys.: Condens. Matter*, 2013, **25**, 345302.

7 S. K. Banerjee, L. F. Register, E. Tutuc, D. Basu, S. Kim, D. Reddy and A. H. MacDonald, *Proc. IEEE*, 2010, **98**, 2032.

8 V. M. Pereira and A. H. C. Neto, *Phys. Rev. Lett.*, 2009, **103**, 046801.

9 F. Schwierz, *Nat. Nanotechnol.*, 2010, **5**, 487.

10 B.-R. Wu, *Appl. Phys. Lett.*, 2011, **98**, 263107.

11 D. Kaplan, V. Swaminathan, G. Recine, R. Balu and S. Karna, *J. Appl. Phys.*, 2013, **113**, 183701.

12 E. V. Castro, K. S. Novoselov, S. V. Morozov, N. M. R. Peres, J. M. B. Lopes dos Santos, J. Nilsson, F. Guinea, A. K. Geim and A. H. Castro Neto, *J. Phys.: Condens. Matter*, 2010, **22**, 175503.

13 S. Tang, J. Yu and L. Liu, *Phys. Chem. Chem. Phys.*, 2013, **15**, 5067.

14 R. Balu, X. Zhong, R. Pandey and S. P. Karna, *Appl. Phys. Lett.*, 2012, **100**, 052104.

15 X. Zhong, Y. K. Yap, R. Pandey and S. P. Karna, *Phys. Rev. B: Condens. Matter Mater. Phys.*, 2011, **83**, 193403.

16 S. Cahangirov, M. Topsakal, E. Aktürk, H. Şahin and S. Ciraci, *Phys. Rev. Lett.*, 2009, **102**(23), 236804; S. Cahangirov, V. O. Özçelik, L. Xian, J. Avila, S. Cho, M. C. Asensio, S. Ciraci and

A. Rubio, *Phys. Rev. B: Condens. Matter Mater. Phys.*, 2014, **90**(3), 035448.

17 Z. Ni, Q. Liu, K. Tang, J. Zheng, J. Zhou, R. Qin, Z. Gao, D. Yu and J. Lu, *Nano Lett.*, 2012, **12**, 113.

18 N. D. Drummond, V. Zólyomi and V. I. Fal'ko, *Phys. Rev. B: Condens. Matter Mater. Phys.*, 2012, **85**, 075423.

19 H. Liu, J. Gao and J. Zhao, *J. Phys. Chem. C*, 2013, **117**, 10353.

20 D. Jose and A. Datta, *Acc. Chem. Res.*, 2014, **47**(2), 593–602.

21 E. Kogan, *Graphene*, 2013, **2**(2), 74–80.

22 E. H. Song, S. H. Yoo, J. J. Kim, S. W. Lai, Q. Jiang and S. O. Cho, *Phys. Chem. Chem. Phys.*, 2014, **16**, 23985; A. Fleurence, Y. Yoshida, C.-C. Lee, T. Ozaki, Y. Y. Takamura and Y. Hasegawa, *Appl. Phys. Lett.*, 2014, **104**, 021605; T. Hussain, S. Chakraborty, A. De Sarkar, B. Johansson and R. Ahuja, *Appl. Phys. Lett.*, 2014, **105**, 123903.

23 S. Lebègue and O. Eriksson, *Phys. Rev. B: Condens. Matter Mater. Phys.*, 2009, **79**, 115409.

24 M. Ezawa, *Phys. Rev. Lett.*, 2012, **109**, 055502.

25 A. Dyrdal and J. Barnas, *Phys. Status Solidi RRL*, 2012, **6**, 340.

26 X. Lin and J. Ni, *Phys. Rev. B: Condens. Matter Mater. Phys.*, 2012, **86**, 075440.

27 H. Sahin and F. M. Peeters, *Phys. Rev. B: Condens. Matter Mater. Phys.*, 2013, **87**, 085423.

28 Y. Liang, V. Wang, H. Mizuseki and Y. Kawazoe, *J. Phys.: Condens. Matter*, 2012, **24**, 455302.

29 Y. Cai, C.-P. Chuu, C. M. Wei and M. Y. Chou, *Phys. Rev. B: Condens. Matter Mater. Phys.*, 2013, **88**, 245408.

30 G. Kresse and J. Furthmuller, *Phys. Rev. B: Condens. Matter Mater. Phys.*, 1996, **54**, 11169; G. Kresse and J. Furthmuller, *Comput. Mater. Sci.*, 1996, **6**, 15; D. Vanderbilt, *Phys. Rev. B: Condens. Matter Mater. Phys.*, 1990, **41**, 7892.

31 G. Kresse and D. Joubert, *Phys. Rev. B: Condens. Matter Mater. Phys.*, 1999, **59**, 1758.

32 P. E. Blochl, *Phys. Rev. B: Condens. Matter Mater. Phys.*, 1994, **50**, 17953.

33 J. P. Perdew, K. Burke and M. Ernzerhof, *Phys. Rev. Lett.*, 1996, **77**, 3865.

34 S. Grimme, *J. Comput. Chem.*, 2006, **27**(15), 1787.

35 R. Zhou, L. C. Lew Yan Voon and Y. Zhuang, *J. Appl. Phys.*, 2013, **114**, 093711.

36 L. Li, X. Wang, X. Zhao and M. Zhao, *Phys. Lett. A*, 2013, **377**, 2628.

37 M. Topsakal, E. Aktürk and S. Ciraci, *Phys. Rev. B: Condens. Matter Mater. Phys.*, 2009, **79**, 115442.

38 K. Saikia, D. Sen, S. Mazumder and P. Deb, *RSC Adv.*, 2015, **5**, 694.

39 A. K. Das and A. J. Thakkar, *J. Phys. B: At., Mol. Opt. Phys.*, 1998, **31**, 2215–2223.

40 K. Anderson and A. J. Sadlej, *Phys. Rev. A: At., Mol., Opt. Phys.*, 1992, **46**, 2356–2362.

11328 | *Phys. Chem. Chem. Phys.*, 2015, **17**, 11324–11328

This journal is © the Owner Societies 2015